

## Comparison of Flow Characteristics of Centrifugal Compressors by Numerical Modelling of Flow

Zvonimir Guzović\*, Mario Baburić, Dubravko Matijašević

*Faculty of Mechanical Engineering and Naval Architecture, University of Zagreb, Ivana Lučića 5, Zagreb, Croatia,*

*\*zvonimir.guzovic@fsb.hr*

---

### Abstract

The centrifugal impellers are used in a wide variety of turbo-machineries, ranging from low pressure fans for cooling of electric motor to high pressure ratio gas turbine compressors, from tiny cryo-cooler compressors to large industrial petrochemical compressor stations. The relative flow in centrifugal impeller is very complex due to different fluid dynamics phenomenon and their interactions. It is subjected to the complex secondary flows and significant separation of the boundary layers, which result in non-uniformity of outlet flow both in tangential direction (e.g. "jet-wake" flow) and axial direction. By the development of experimental and computational techniques the considerable progress in understanding of complex flow effects in impeller is made.

The wide-spread use of reactive impellers with backswept blades in all state-of-the-art designs of compressors has resulted in significant improvements of aero and thermodynamics characteristics of impeller (e.g. distribution of outlet flow velocities).

The increasingly present appearance in the several recent years of calculations by means of verified and validated users software based on the engineering numerical methods enables an increasingly wide replacement of time-consuming experimental investigations (i.e. of physical modelling), which give a limited number of data of integral character, by mathematical modelling which gives a large number of data over a short time, enabling not only integral but also structural analysis. This results in rapid and significant improvements of aero and thermodynamics characteristics and in the end in energy conversion efficiency.

The aim of the paper is to apply expert knowledge in carrying out numerical modelling of the flow in centrifugal compressor by means of users software. The algorithm is presented on the comparison of aero and thermodynamics characteristics of centrifugal compressors with reactive impellers with backswept normal and "S" shape blades. The comparison shows that the compressor with impeller with "S" shape blades has better aero and thermodynamics characteristics and thus also the energy conversion efficiency. Since there are experimental measurements of aero and thermodynamics characteristics of the numerically investigated compressors in literature, the verification and validation of the users software have been performed simultaneously. Also the alternating modelling of the flow and change of impeller blades geometry with the aim of improving the aero and thermodynamics characteristics up to attaining of maximum possible efficiency of energy conversion presents the algorithm of geometry optimisation of the impeller design with backswept blades.

---

### Introduction

The centrifugal compressors are widely used in a variety of applications because of their ability to achieve high pressure ratios in a relatively short axial distance and due to their rugged construction.

In designs of stationary compressors, with medium values of circumferential velocity (up to  $u=300$  m/s), the centrifugal impellers with radial inlet of flow on the

blades are applied. Usually, with such impellers the exit angle of blades is  $\beta_2 < 90$  deg and they are conditionally named reactive. In design of compressors e.g. dedicated to the charge of internal combustion engines and in smaller power gas-turbine plants, which feature significant circumferential velocities (about  $u=500$  m/s), due to the strength conditions the impellers are performed with axial inlet of flow on blades (i.e. axial-radial impellers). In many cases such impellers are designed

**Nomenclature**

$c_p$  - specific heat at constant pressure, J/kgK;  
 $D$  - diameter, m;  
 $f$  - rotational frequency, s<sup>-1</sup>;  
 $k$  - thermal conductivity, W/mK;  
 $\dot{m}$  - mass flow rate, kg/s;  
 $p$  - pressure, Pa;  
 $R$  - radius, m;  
 $r$  - compression (pressure) ratio, -;  
 $T$  - temperature, K;  
 $u$  - circumferential velocity, m/s;  
 $z$  - number of impeller blades, -;

Greek Letters

$\beta'$  - impeller blade angle, deg;  
 $\eta$  - isentropic efficiency, -;  
 $\mu$  - dynamic viscosity, kg/m s;  
 $\rho$  - mass density, kg/m<sup>3</sup>;

Subscripts

in - inlet;  
 out - outlet;  
 nom - nominal value;  
 ref - reference value;  
 hub - at hub of impeller;  
 tip - at tip of blade;  
 conv - convex surface of impeller blade;  
 conc - concave surface of impeller blade;  
 0 - total pressure;  
 1 - impeller inlet;  
 2 - impeller outlet;  
 3 - vaneless diffuser outlet;  
 4 - spiral casing outlet;

with exit angle of blades  $\beta'_2 < 90$  deg. On the other hand, the axial-radial impellers are usually performed due to manufacturing simplicity as impellers with  $\beta'_2 = 90$  deg, with inducer which represents the axial cascade in which the blade incline angle is increased from  $\beta'_1$  (on inlet) to  $\beta'_1 = 90$  deg (on exit). In this part of impeller the directrices of the blade surface are directed along the radius. In the radial part of the impeller, due to the realization of the exit angle  $\beta'_2 < 90$  deg, the blade is curved round the circular arc in the plane of rotation, while its surface is also linear with direction of blades directrices parallel to the axis, Fig. 1, impeller 2a. The blade incline angle in this part of impeller is changed from  $\beta' = 90$  deg to the value of the exit angle  $\beta'_2$ . In the region between the axial and the radial part of the impeller, i.e. in the area of transition from axial to radial direction, the blade incline angle equals 90 deg.

In such design of blades of the reactive impeller (called impeller with normal blades or «the first type impeller») their shape and consequently the shape of channels is less favourable than in impellers with radial blades ( $\beta'_2 = 90$  deg) and more than in case of reactive impeller with radial inlet of flow on blades. With such shape of blade the angle of its incline in the change from  $\beta'_1$  to  $\beta'_2$  assumes also the value  $\beta' = 90$  deg, resulting in the change of sign of the blade lateral surface curvature. In these conditions the advantages of reactive impeller are annulled due to the increase in losses, caused by this shape of the blade. Due to the decrease in losses in the centrifugal reactive impeller with axial inlet of flow on blades it is necessary to insure monotonous change of blade incline angle from  $\beta'_1$  to  $\beta'_2$ , i.e. without assuming the value  $\beta' = 90$  deg. The blade shape also changes monotonously along the entire length, without the change of sign of the curvature of its lateral surface.

The centrifugal impellers of this type are applied in pumps, where the direction of inlet of flow on the blades is close to axial. The blade surface of impeller of this pump has curvilinear directrices, which significantly complicates their manufacturing. Due to the simplicity of manufacturing of the reactive axial-radial impeller with monotonous change of angle  $\beta'$ , it is desirable to preserve the blade surface straight, i.e. that the blade surface has straight directrices, which are at a certain angle to the impeller axis and intersect it. In this case the blade surface has the shape of a screw surface or simply the "S" shape, with directrices directed along the normal to the middle line of the impeller meridional section, Fig. 1, impeller 2b (called impeller with "S" shape blades or "the second type impeller").

One of the methods of determining the optimal surface shape of "S" blade, i.e. of change of the blade incline angle from  $\beta'_1$  to  $\beta'_2$  is by means of experimental investigation. Unfortunately the experimental investigations are time-consuming and the limited number of obtained data is most frequently of integral character. Therefore, the design optimization of the impeller blades with the aim of improving the aero and thermodynamics characteristics, i.e. efficiency of energy conversion is adequately slow. Fortunately, the recent increasingly present appearance of calculations by means of user software based on the verified and validated engineering numerical methods enables an increasingly wide replacement of experimental investigations (i.e. of physical modelling) by mathematical modelling. These methods enable not only structural but also integral analysis of the flow and energy conversion processes in the impeller. A large number of data obtained over a short time results in rapid and significant improvements of aero and thermodynamics characteristics, and eventually in the energy conversion efficiency.

The paper presents the algorithm of numerical modelling of flow in the centrifugal compressor, based on the application of expert knowledge and the usage of user software. The algorithm is presented on the comparison of aero and thermodynamics characteristics of centrifugal compressors with reactive impellers with backswept normal and "S" shape blades whose geometries and results of experimental investigations are presented in literature [1]. Thus it was possible to simultaneously perform the verification and validation of the users software.

In principle the algorithm serves for optimization of the impeller design, i.e. improvement of its aero and thermodynamics characteristics and thus also the processes of energy conversion with the aim of attaining maximum possible isentropic efficiency. The first step in the optimization process of impeller design is obtaining the initial three-dimensional geometry on the basis of results of aero and thermodynamics calculations and other empirical data by means of the graph-analytic method fully automated on the computer [2], [3]. The obtained impeller geometry can be considered as «well-designed». The final (optimal) geometry is obtained after a definite number of iterations between numerical calculations (modelling) of flow and changes of geometry of impeller blades. The optimal geometry assumes these aero and thermodynamics characteristics of flow in impeller which result in maximum possible isentropic efficiency.

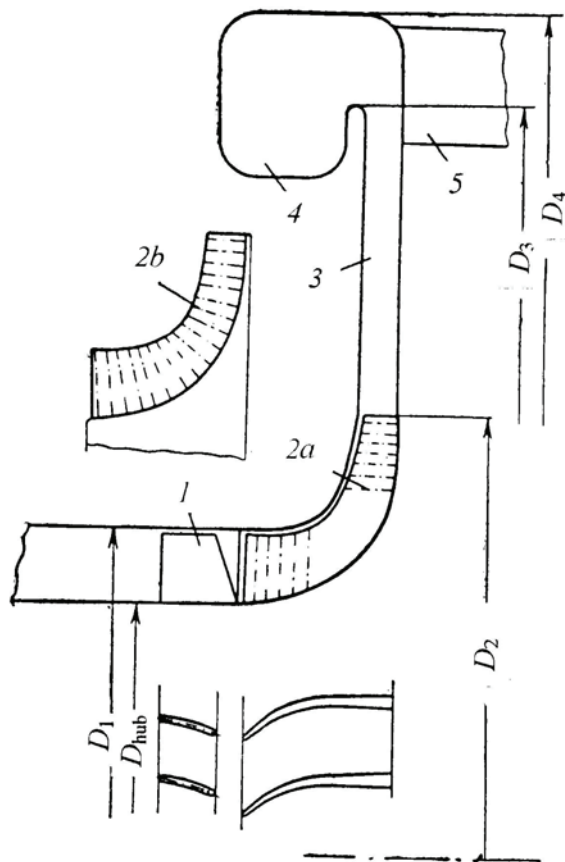


Fig. 1. The scheme of investigated compressor: 1-inlet guide vanes; 2a, 2b-impeller with "normal" i.e. "S" shape blades; 3-vaneless diffuser; 4-spiral casing; 5-connection

## Flow behaviour in impeller

The impellers of centrifugal compressors are characterized by long three-dimensional blade channels with high curvature. The blades make 90 deg turn in the meridional plane and have opposite angle turns in inlet axial part (the inducer) and exit radial part (the exducer). In the inducer the blade angle with respect to the tangent direction increases, thus allowing the pressure rise through internal flow diffusion. In the exducer where blade loading is dominated by Coriolis forces, the blade angle is reduced in order to prevent excessive loading.

The real flow that develops in centrifugal impeller, under the combined effects of deceleration, Coriolis force and meridional curvature, and which simultaneously acts on the boundary layers on channels walls, is very complex [4], [5], [6]. The Coriolis force component perpendicular to the rotating blade surface influences the boundary layer stability: on the blade suction side the turbulence production is inhibited and the boundary layer becomes prone to separation. Due to the complex transition of the flow and rotational forces, strong secondary flows are produced. These secondary flows, along with separated flow regions, lead to strong crossflow velocity components, which transport the fluid with low momentum and high total-pressure loss into the mainstream. Also in unshrouded impellers the interaction of the low-momentum fluid in the boundary layer with the tip leakage flows is significant.

First of all, the complex secondary flows and significant boundary layer separation, as well as the interaction of the low-momentum fluid in the boundary layer with the tip leakage flows result in the impeller outlet flow non-uniformity in which the low-velocity wake region is close to the suction surface and jet region near the pressure surface of the blade. This flow pattern is called the "jet-wake" flow [5], [6]. The mixing of this "jet-wake" flow is the source of significant loss generation. The outlet flow velocity field is non-uniform both in circumferential (pitchwise) and in axial (spanwise) direction. While the circumferential variations in the outlet flow level up very rapidly, at the same time the axial variations in the flow seem to persist well into the diffuser. This axial flow variation has an adverse effect on the pressure recovery of the diffuser (vaned or vaneless) and it is one of the main causes of stage instability in compressors. Therefore, the minimization or possible suppression of the formation of the outlet flow non-uniformity should not only lead to substantial improvement in stage performance but also result in increases in the stable operating range of the turbomachine.

In order to design impellers with a more uniform outlet flow field, it is important to understand the basic mechanisms behind the generation of the outlet flow non-uniformity and then produce appropriate design guidelines to minimize their effects by changes to the impeller geometry [3].

The dominant influence of secondary flows on the generation of the "jet-wake" flow has been known for as

many as about forty years [4], [5], [6]. The use of blade lean or spanwise stacking (i.e. of “S” shape blade) can minimize the secondary flows in the impeller and obtain a more uniform outlet flow field. The use of excessive amounts of blade lean, however, can result in structural problems or manufacturing difficulties.

**Presentation of experimental investigations results**

Fig. 1 presents the scheme of experimental stage from [1] at which the experimental investigations of both impellers have been carried out. The stage consists of inlet guide vanes which give to the flow on in the impeller inlet a certain pre-whirl, of reactive impeller with backswept normal (“the first type impeller”) or “S” shape (“the second type impeller”) blades, of vaneless diffuser of relatively large length in radial direction and of spiral casing with two connections, which turn the flow in axial direction. The stage with “the first type impeller” features the following design values and geometrical characteristics:  $u_{2nom}= 341$  m/s;  $f_{nom}= 586.67$  s<sup>-1</sup>;  $p_{in0}= 103,300$  Pa;  $T_{in}= 288$  K;  $D_2= 185$  mm;  $D_1/D_2= 0.729$ ;  $D_{hub}/D_1= 0.785$ ;  $D_3/D_2= 1.7$ ;  $D_4/D_2= 1.915$ .

Fig. 2 denotes with *a* “the first type impeller”, and Table 1 gives the blade geometry by means of coordinates of its concave and convex surfaces. The number of impeller blades is  $z= 27$ . The inducer inlet angles on diameters  $D_1$  and  $D_{hub}$ :  $\beta_{1,tip}= 44$  deg and  $\beta_{1,hub}= 51$  deg. Along the inducer, on all sections the angles increase up to  $\beta= 90$  deg. On the radial part in rotational surface the blade is curved along the circle arc with the radius of  $R= 26.7$  mm. The exit blade angle  $\beta_2= 61.01$  deg.

Fig. 2 denotes with *b* “the second type impeller”, and Table 2 gives the blade geometry by means of

coordinates of its concave and convex surfaces. It has in the meridional section the same shape as «the first type impeller», also the same number of blades  $z$  and exit blade angle  $\beta_2$ . The values of inducer inlet angles are somewhat lower ( $\beta_{1,tip}= 38$  deg and  $\beta_{1,hub}= 45$  deg).

The experimental investigations of the stage with both types of impeller are carried out with total pressure on inlet  $p_{in0}= 1$  bar and  $p_{in0}> 1$  bar. At the inlet into the stage for measuring the air flow, the measuring collector with 100 mm diameter is built in. Between the collector and the investigated stage the diffuser with divergence angle of 8 deg is installed. The total pressure of air on the stage inlet is measured at five points by the measuring devices for total pressure and the temperature by resistance thermometer, installed in pipe before the measuring collector. The measurement results of total pressure on inlet are arithmetically averaged.

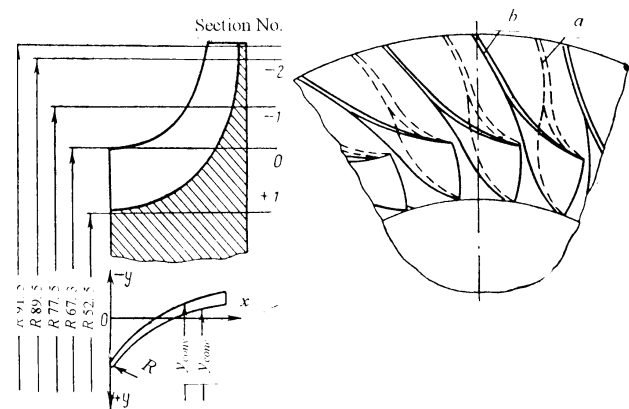


Fig. 2. The reactive impellers with backswept normal (a) and “S” shape (b) blades

Table 1. The blade geometry of “the first type impeller” (coordinates of concave and convex surfaces)

Section No.	X	0	3.5	7	9.5	12	14.5	16	17	19	21	23	25	27	29	31	R
1	$y_{conv}$	6.34	3.56	1.48	0.36	-0.47	-1.00	-1.19	-1.2								0.43
	$y_{conc}$	7.35	5.09	3.26	2.30	1.66	1.30	1.24	1.2								
0	$y_{conv}$	8.45	5.00	2.39	1.00	0	-0.64	-0.89	-0.9	-0.97	-1.05	-1.13	-1.20	-1.28	-1.35	-1.43	0.25
	$y_{conc}$	9.12	6.12	3.71	2.43	1.52	1.02	0.91	0.9	0.97	1.05	1.13	1.20	1.28	1.35	1.43	
-1	$y_{conv}$								-0.7	-0.78	-0.85	-0.93	-1.00	-1.08	-1.15	-1.23	
	$y_{conc}$								0.7	0.78	0.85	0.93	1.00	1.08	1.15	1.23	
-3	$y_{conv}$									-4.30	-4.39	-4.47	-4.56	-4.64	-4.73	-4.81	
	$y_{conc}$									-3.68	-3.59	-3.51	-3.42	-3.34	-3.25	-3.17	

Table 2. The blade geometry of “the second type impeller” (coordinates of concave and convex surfaces)

Section No.	x	0	2.5	5	7.5	10	12.5	15	19	21	23	25	27	31	R
1	$y_{conv}$	9.23	6.35	4.75	3.60	2.70									0.43
	$y_{conc}$	10.12	8.32	7.15	6.04	5.18									
0	$y_{conv}$	11.10	7.34	4.20	1.90	0.15	-1.33	-2.56	-4.20	-4.87	-5.47	-6.00	-6.50		0.25
	$y_{conc}$	11.87	8.60	5.95	4.05	2.36	0.90	-0.48	-2.00	-2.63	-3.12	-3.50	-4.00		
-1	$y_{conv}$								-11.03	-11.46	-11.8	-12.13	-12.41	-12.81	
	$y_{conc}$								-8.97	-9.31	-9.57	-9.78	-9.96	-10.24	
-2	$y_{conv}$										-21.06	-21.16	-21.27	-21.63	
	$y_{conc}$										-20.31	-20.20	-20.10	-20.01	

The measurements results of the total pressure and temperature after the stage are carried out in exit collector at sixteen points. The measurements of total pressure and total temperature on exit are also arithmetically averaged.

The compressor stage is driven by direct current electric motor. In the course of investigations the power delivered to shaft of compressor stage is determined. This is enabled the calculation of compressor isentropic efficiency both by the delivered power and by the temperatures.

The compression ratio  $r = 1.85$  and the isentropic efficiency  $\eta = 0.7$  are determined by the mass flow  $\dot{m} = 0.7$  kg/s and rotational frequency  $f = 586.67$  s<sup>-1</sup> at stage with “the first type impeller” on the basis of the measurement results. Simultaneously, the same quantities for stage with “the second type impeller” have been obtained about 11% higher. On the basis of this, the authors [1] have concluded that the obtained improvement of characteristics of stage with “the second type impeller” is based on the increase of impeller efficiency. They explain the latter by more favourable blades shape and consequently the impeller channels, which decreases the losses in impeller. The losses are decreased due to the reduction of blade turning angle, reduction of relative velocities gradient in inlet part of impeller and due to monotonous change of blade lean along the length and keeping of curvature sign of the blade surface unchanged.

The complete interpretation of previous results will be given by the numerical modelling of the flow in compressors with the described “first and second type impeller”, which are presented in the next chapter.

### Investigation of compressors by numerical modelling of flow

On compressors with both type of impellers, whose geometry and results of experimental investigations of aero and thermodynamics characteristics are presented in previous chapters from [1], now the same investigations are performed by numerical modelling of flow.

#### Discretisation of geometrical domain by the grid of finite volumes

Before the very numerical simulation in CFD (Computational Fluid Dynamics) user software, the discretisation of geometrical investigated domain has been made; in this case by grid of the finite volumes. The grid of the finite volumes coincides with the geometrical domain. The domain in this case represents the configuration of inlet guide vanes, reactive impeller with normal (“the first type impeller”) or “S” shape (“the second type impeller”) backswept blades and vaneless diffuser. Due to the periodic rotational symmetry of configuration of inlet guide vanes, the impeller and vaneless diffuser it is sufficient to model the flow in one segment of impeller, and downstream in one segment of inlet guide vanes and upstream in one segment of

vaneless diffuser by the application of adequate boundary conditions on boundaries of rotational symmetry. The segment of impeller is extended between symmetrals of two neighbouring channels with the blade in the middle. It is similar to the downstream located segment of inlet guide vanes which is also extended between the symmetrals of two neighbouring channels with stator blade in the middle, while the segment of vaneless diffuser with width which is equal to the exit width of the impeller channel is located upstream. With this, the necessity for processor and memory power of computer in the course of CFD simulation is significantly reduced, enabling the usage of grid of finite volumes of higher density than in the case of the entire physical domain modelling. For the creation of the grid of finite volumes the user software GAMBIT was used.

Since in the domain, one part rotates (impeller), and the other two parts rest (inlet guide vanes and vaneless diffuser), the separated grids of finite volumes are made for these particular parts of domain. The first is the made part of the domain of inlet guide vanes segment which is equal in both modelled cases, and then the other two parts of domain, the segments of impeller and of the vaneless diffuser, for both types of impellers. Before numerical calculation the different parts of domain are combined in the user software FLUENT in a single complete domain with clearly defined interface.

The finite volume grid for the compressor with “the first type impeller” is presented in Fig. 3, and for the compressor with “the second type impeller” in Fig. 4.

In the first case the domain is discretised with 277,740 finite volumes, and in the second case with 221,376 finite volumes. In both cases the grids are completely made of finite volumes shaped as hexahedron.

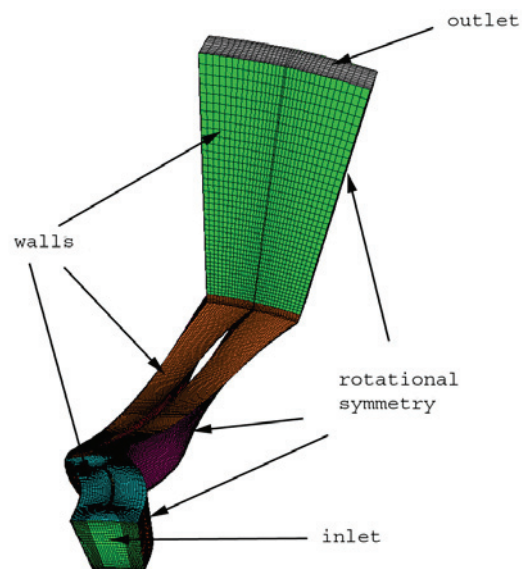


Fig. 3. The finite volume grid for the compressor with “the first type impeller”



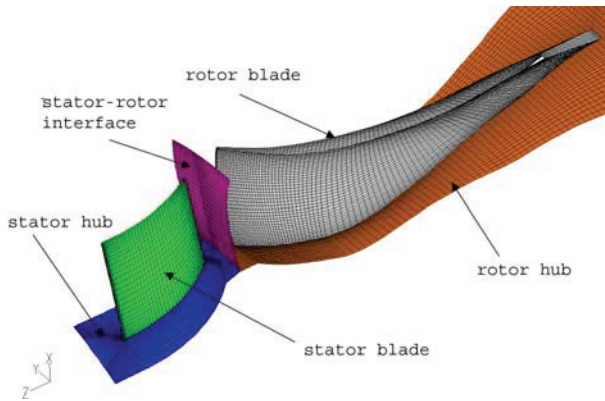


Fig. 4. The finite volume grid for the compressor with “the second type impeller” (part)

### Numerical calculation

For complete defining of the mathematical model used in numerical calculations it is necessary to set the boundary conditions on the boundary surfaces of the domain, which describe the physical conditions on domain boundaries. In this numerical calculation there are unambiguously defined boundary surfaces of the domain: inlet and outlet surface, surfaces of stator and rotor blades, walls of disc, impeller hub and inducer hub, surfaces of rotational symmetry and interfaces. Figs. 3 and 4 present a domain with the defined boundary surfaces.

On the inlet surface the mass flow of air  $\dot{m} = 0.026$  kg/s, inlet temperature  $T_{in} = 288$  K and inlet pressure  $p_{in} = 100,000$  Pa have been set. On the outlet surface the outlet pressure  $p_{out} = 185,000$  Pa (i.e. “pressure outlet”) has been set. In all the walls the adiabatic boundary condition is used, and with stationary walls (inlet guide vanes, shroud, vaneless diffuser) the rotational frequency is set  $f = 0$  and at the impeller wall the rotational frequency round the axial axis  $f = 586.67$  s<sup>-1</sup>. On the surface of rotational symmetry the boundary condition of rotational symmetry is used.

The working fluid is air whose density is calculated by equation for ideal gas. Also, the following physical properties are used in calculations: specific heat at constant pressure  $c_p = 1006.43$  J/kgK; thermal conductivity  $k = 0.0242$  W/mK; viscosity  $\mu = 1.7894 \cdot 10^{-5}$  kg/sm. The reference pressure is taken  $p_{ref} = 100,000$  Pa.

The numerical calculation is performed in CFD user software FLUENT. Since in the domain one part rotates (impeller) and the other two rest (inlet guide vanes and vaneless diffuser), it is not possible to perform the stationary simulation provided the consistence of the mathematical model with real physical state is maintained. Therefore, the numerical calculation is performed by means of non-stationary mathematical model, which takes into consideration the relative movement between inlet guide vanes and the impeller, as well as between the impeller and the vaneless diffuser (i.e. sliding mesh).

Other characteristics of the numerical calculations are:

- the non-stationary, three-dimensional solver, with non-conjugate solution of main equations and absolute formulation of velocity has been used;
- along with standard  $k-\varepsilon$  turbulence model, also the standard wall functions for modelling of viscose layer near the wall are used;
- in energy calculation the enthalpy equation, assumption of adiabatic walls and fluid heating close to wall due to viscose friction (option of viscose heating) are included;
- from the numerical theses the following are used: the Simple algorithm of velocity and pressure conjugation, the second order upwind scheme as discretisation method and sub-relaxation factors;
- the equations of flow, turbulence and energy (enthalpy) are solved;
- the time interval is chosen so that in calculation 50 time intervals for one period are needed, i.e. that the relative position of impeller towards the inlet guide vanes and vaneless diffuser is equal to the initial one;
- the calculation is completed when the calculation results start to be repeated periodically.

### The results of numerical modelling of flow

Figs. 5 – 18 present the results of numerical modelling of flow in centrifugal compressors with «the first and second types of impellers.

In both cases the sufficiently uniform distributions of absolute pressure along impeller channels are observed, Figs. 5 - 6. Obviously, the distributions of density are visually similar to distributions of absolute pressure, Figs. 7 - 8, because these two quantities are directly related by the state equation of ideal gas and they are proportional. The temperature distributions for both cases are presented in Figs. 9 - 10. Similarly as with the previous two quantities, the temperature distributions are uniform, and clearly visible areas of increased temperature are close to the walls, which results in the viscose friction close to the walls. The distributions of relative velocities for both types of impellers are presented in Figs. 11 - 12. In Fig. 11 in case of “the first type of impeller” an area near the shroud is observed, which starts from the location of transition from axial to radial direction, of accumulation of low momentum fluid and with high losses. This is explained by the intensive secondary flow which displaces the low momentum fluid toward shroud (i.e. toward casing), and which is, as other investigators have indicated, characteristic for impellers with axial inducer [5], [6]. As shown in Fig. 12, with “the second type of impeller”, the existence of the secondary flows is not observed at all. Therefore it may be concluded that the replacement of normal blades by “S” shape blades effectively eliminates the occurrence of the secondary flows.

The distributions of Mach numbers for both types of impellers are presented in Figs. 13 - 14. From the distributions it is possible to conclude that in the region of the inducer, near the inlet edge toward the periphery of

blades the values of Mach number are increased, but still below the critical ones, which positively influences the stability of boundary layers.

The distributions of relative velocities on the radius  $R=0.075$  m (Figs. 15 - 16) and in outlet section (Figs. 17-18) for both types of impellers are especially illustrative. At first sight it may be observed that in both sections the distributions of relative velocities with “the second type of impeller” are more uniform (Figs. 15 and 17) than with “the first type of impeller” (Figs. 16 and 18). However, it should be noted that in neither type of impeller in the outlet sections the “jet-wake” is not present, only with “the first type of impeller” it is possible to speak about its almost negligible presence. The distributions of velocities both in axial and in circumferential direction are satisfactorily uniform, especially with “the second type of impeller”. This contributes to effective diffuser operation, which is confirmed by Figs. 5-6, where significant pressure increase is observed with uniform distribution. All this tells about the positive influence of the usage of reactive impellers with the aim of preventing the flow non-uniformity at the outlet from impeller, i.e. of “jet-wake” flow, especially of “the second type of impeller”.

On the basis of calculation results of temperatures and pressures during one period the isentropic efficiency has been calculated. The values of isentropic efficiency during one period for compressor with “the first type of impeller» are presented in Fig. 19, while the same for compressor with “the second type of impeller” are presented in Fig. 20. The average value of isentropic efficiency during one period for compressor with “the first type of impeller” is  $\eta = 0.784$ , while for compressor with “the second type impeller” is  $\eta = 0.85$ . Generally, the numerical modelling has yielded higher values than by experimental measurements, but the mutual difference is 10% as well as with experimental measurements. The obtained higher value of isentropic efficiency in compressors with impeller with “S” shape blades than with compressors with impeller with normal blades can be explained by the fact that with the impeller with “S” shape blades the secondary flow is almost eliminated. This is also indicated with the attained average values of pressure ratios:  $r = 1.855$  versus  $r = 1.812$ . The first value is equal to the value obtained during experimental measurements, and the second value is 2% lower.

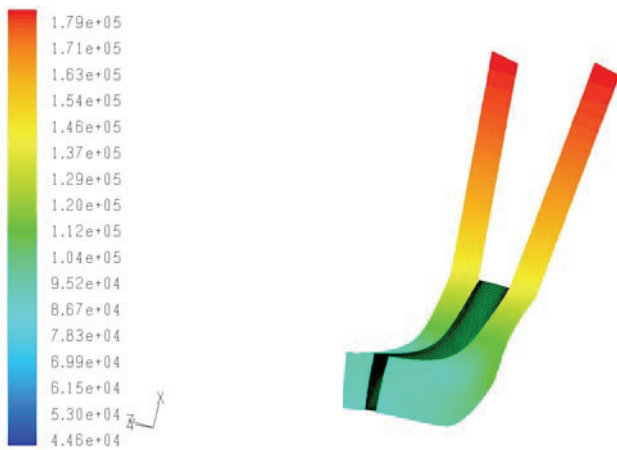


Fig. 5. Distribution of absolute pressure along compressor with “the first type of impeller”

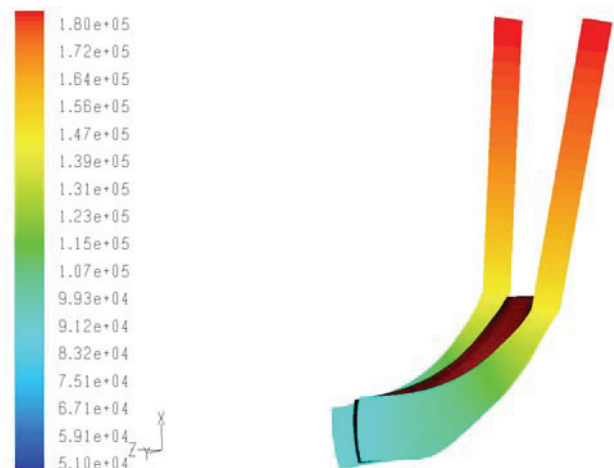


Fig. 6. Distribution of absolute pressure along compressor with “the second type of impeller”

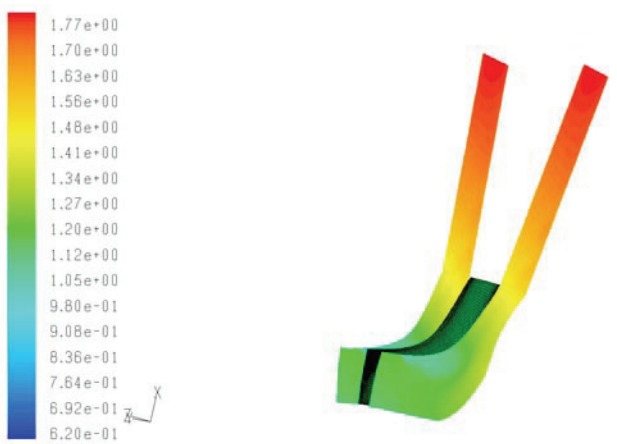


Fig. 7. Distribution of density along compressor with “the first type of impeller”

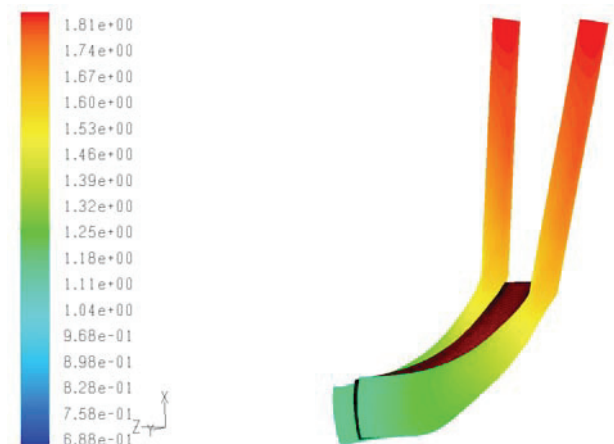


Fig. 8. Distribution of density along compressor with “the second type of impeller”

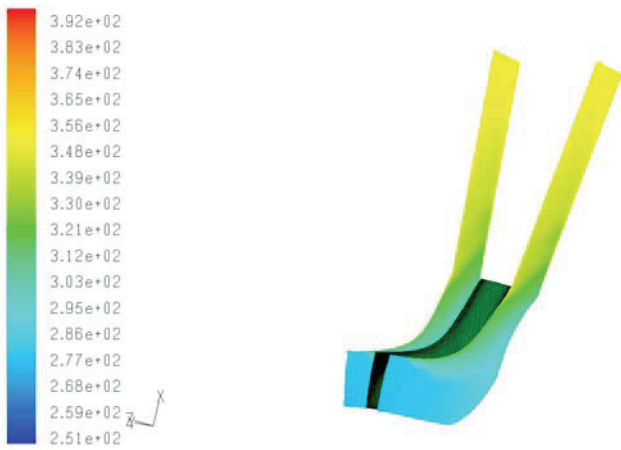


Fig. 9. Distribution of temperature along compressor with "the first type of impeller"

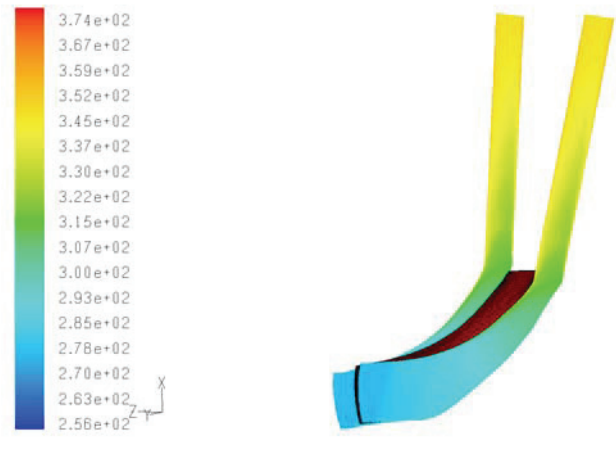


Fig. 10. Distribution of temperature along compressor with "the second type of impeller"

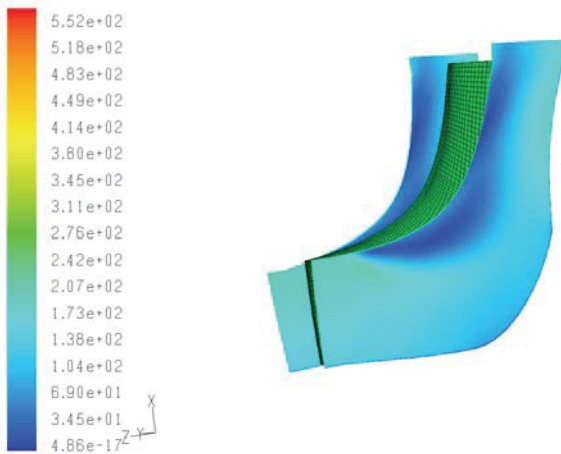


Fig. 11. Distribution of relative velocity along "the first type of impeller"

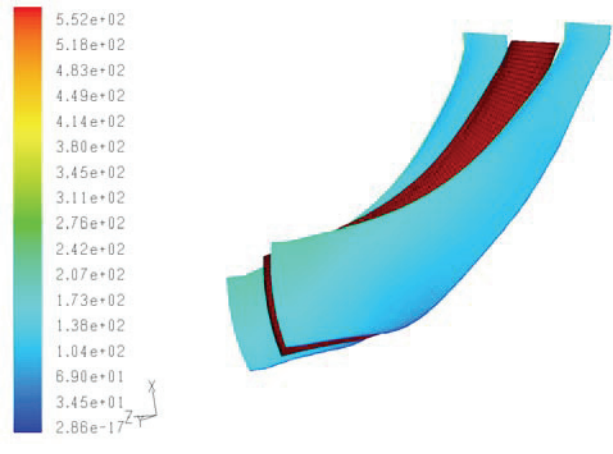


Fig. 12. Distribution of relative velocity along "the second type of impeller"

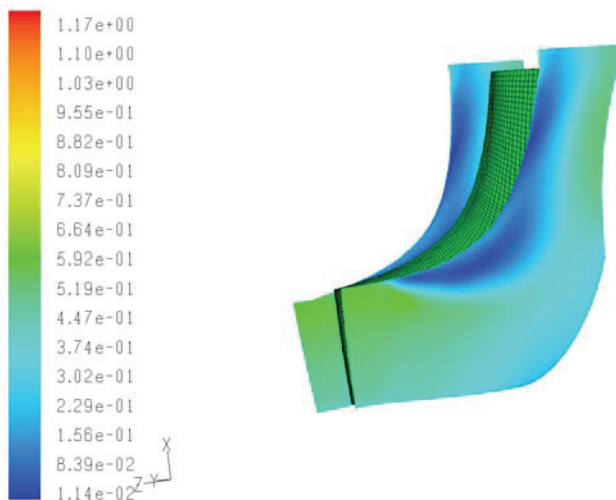


Fig. 13. Distribution of relative Mach number along "the first type of impeller"

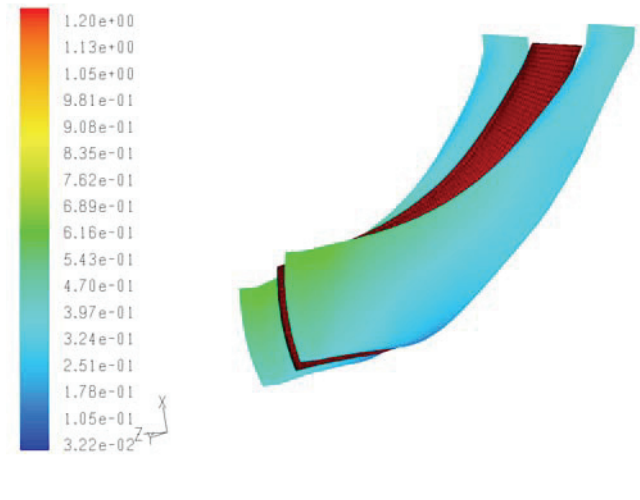


Fig. 14. Distribution of relative Mach number along "the second type of impeller"



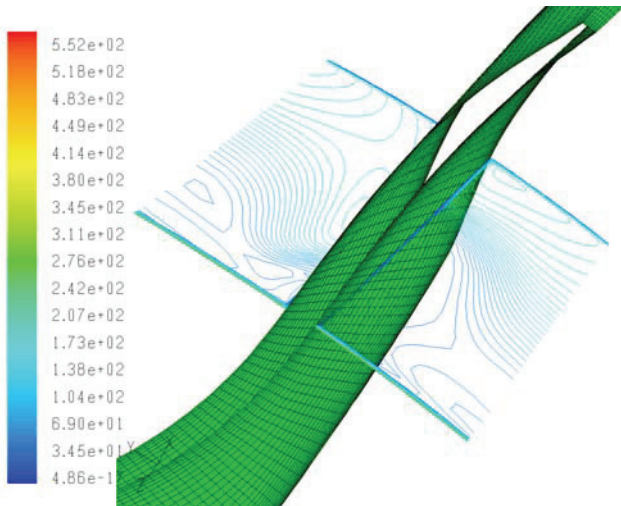


Fig. 15. Distribution of relative velocity at “the first type of impeller” on  $R= 0.075\text{m}$

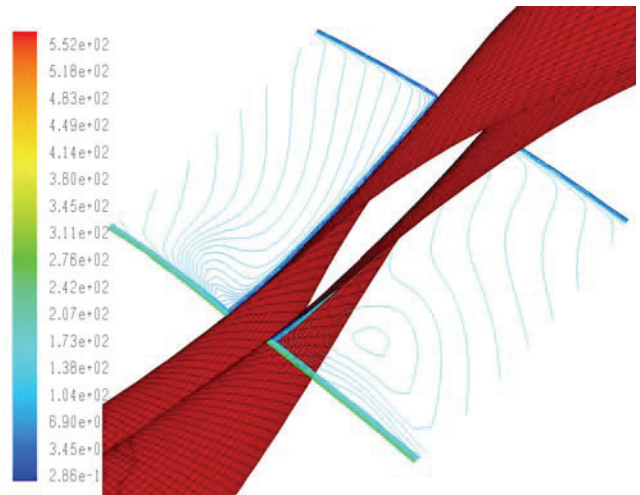


Fig. 16. Distribution of relative velocity at “the second type of impeller” on  $R= 0.075\text{m}$

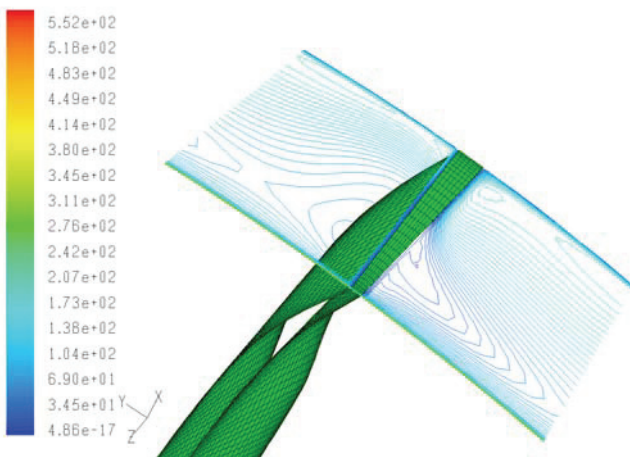


Fig. 17. Distribution of relative velocity at “the first type of impeller” in outlet section

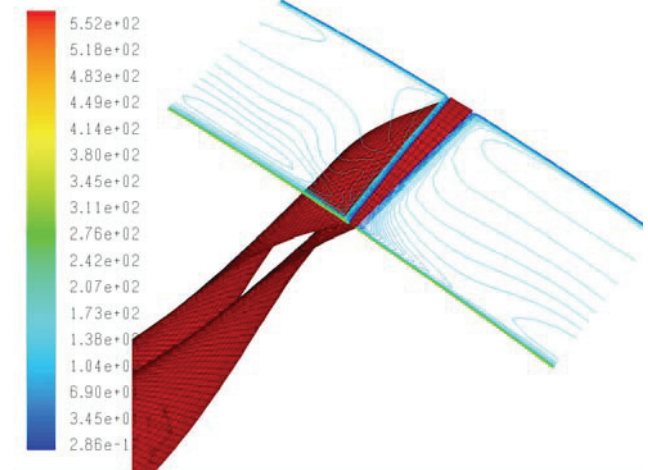


Fig. 18. Distribution of relative velocity at “the second type of impeller” in outlet section

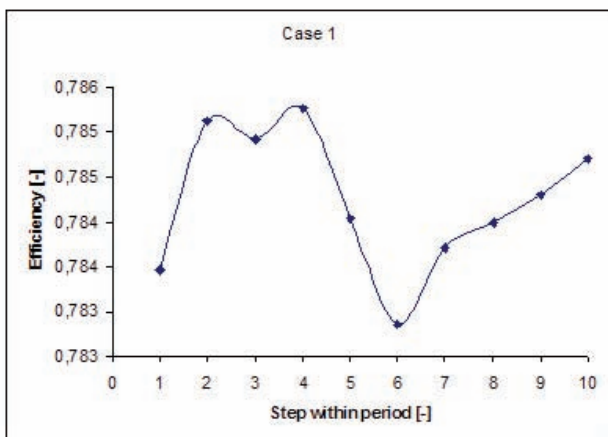


Fig. 19. The values of isentropic efficiency during one period for compressor with “the first type of impeller”

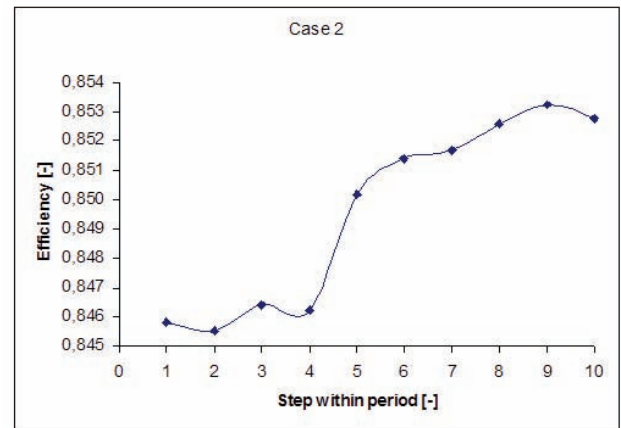


Fig. 20. The values of isentropic efficiency during one period for compressor with “the second type of impeller”

## Conclusion

The paper presents the possibility of investigating the flow phenomenon in centrifugal compressor by means of verified and validated user software and of required expert knowledge. The algorithm of numerical modelling of flow is presented in comparison of flow characteristics and efficiencies of compressors with two types of reactive impellers with backswept blades, with normal blades and "S" shape blades. The better is the compressor with impeller with "S" shape blades: as the numerical modelling of flow shows, it almost completely eliminates secondary flows and the calculation of efficiency gives efficiency higher by about 10%. It can be concluded that both types of reactive impellers effectively prevent the flow non-uniformities on the outlet from impellers, i.e. the "jet-wake" flow is almost inexistent on impellers outlets. Since the experimental measurements exist for the modelled compressors, it was possible to carry out the verification and validation of user software. The agreement between the results obtained by numerical modelling and by experiments is satisfactory, which enables complete replacement of the time-consuming experimental investigations by much rapid numerical simulations.

The represented numerical modelling of flow in centrifugal compressor makes it possible to carry out the optimisation of basic part of compressor (e.g. impeller) with the aim of improving the efficiency of machinery. Based on the results of numerical calculations, the correction of design is made with the aim of improving the flow characteristics, i.e. of energy conversion process, until achievement of maximum possible efficiency.

## References

- [1] I.A. Gurvich, L.L. Levaschov, M.H. Etingof, Results of experimental investigation of centrifugal compressor stage, (in Russian), *Teploenergetika* (2) (1980) 34-38.
- [2] Z. Guzovic, B. Matijasevic, I. Novko, CAD Modelling of the Optimal Axial-Radial Impeller of the Centrifugal Compressor for CAM, Proceedings of the 10th International DAAAM Symposium, Ed. B. Katalinic, Vienna, (1999) 175-176.
- [3] B. Matijasevic, K. Horvat, Z. Guzovic, Design Optimization of Centrifugal Compressor Impeller by Numerical Modelling, Proceedings of the 6th International Research/Expert Conference TMT 2002, Eds. S. Brdarevic, S. Ekinovic, R. Compamys, J. Vivancos, Neum, Bosnia and Herzegovina, (2002) 413-416.
- [4] M.D. Hathaway, R.M. Chriss, J.R. Wood, A.J. Strazisar, Experimental and Computational Investigation of the NASA Low-Speed Centrifugal Compressor Flow Field, *Journal of Turbomachinery*, 120 (1993) 527-542.
- [5] M. Zangeneh, Inviscid-Viscous Interaction Method for Three-Dimensional Inverse Design of Centrifugal Impellers, *Journal of Turbomachinery*, 120 (1994) 280-290.
- [6] M. Zangeneh, A. Goto, H. Harad, On the Design Criteria for Suppression of Secondary Flows in Centrifugal and Mixed Flow Impellers, *Journal of Turbomachinery*, 120 (1998) 723-735.